

Article

Numerical Optimization Study of the Resistance Coefficient of U-Shaped Air Distributor

Zhijing Wu¹, Jinfeng Wang^{1,2,3,4}  and Jing Xie^{1,2,3,4,*} 

¹ College of Food Science and Technology, Shanghai Ocean University, Shanghai 201306, China; 2035207@st.shou.edu.cn (Z.W.); jfwang@shou.edu.cn (J.W.)

² Shanghai Professional Technology Service Platform on Cold Chain Equipment Performance and Energy Saving Evaluation, Shanghai 201306, China

³ National Experimental Teaching Demonstration Center for Food Science and Engineering, Shanghai Ocean University, Shanghai 201306, China

⁴ Quality Supervision, Inspection and Testing Center for Cold Storage and Refrigeration Equipment, Ministry of Agriculture, Shanghai 201306, China

* Correspondence: jxie@shou.edu.cn; Tel.: +86-156-9216-5513

Abstract: In this paper, the optimization of the flow channel structure of the U-shaped air distributor is proposed. Fluent meshing was used to mesh the multipatch meshing of the original model of the grid air distributor, and then the CFD numerical simulation was carried out by using Fluent 2022R1 to obtain the internal air flow state of the air distributor flow channel. Through the orthogonal experimental design and a comprehensive analysis method, the optimal size structure for resistance performance is obtained as $S = 60$ mm, $RL = 125$ mm, $L = 160$ mm, $D = 100$ mm, the resistance coefficient of the new structure as 1.375, and the pressure loss as 56.87 Pa, by using 3D modeling software (SOLIDWORKS 2015) and Fluent. Compared with the initial scheme, the resistance coefficient and pressure loss are reduced by 3.03% and 6.29%, respectively. To summarize, the research in this paper offers a substantial contribution to the realm of energy conservation and emission abatement in ship air conditioning systems, simultaneously furnishing invaluable guidance for the design of air distributors.



Citation: Wu, Z.; Wang, J.; Xie, J. Numerical Optimization Study of the Resistance Coefficient of U-Shaped Air Distributor. *Processes* **2023**, *11*, 2405. <https://doi.org/10.3390/pr11082405>

Academic Editors: Wei Cai, Yan Wang, Zhigang Jiang and Yue Wang

Received: 10 July 2023

Revised: 4 August 2023

Accepted: 7 August 2023

Published: 10 August 2023



Copyright: © 2023 by the authors. Licensee MDPI, Basel, Switzerland. This article is an open access article distributed under the terms and conditions of the Creative Commons Attribution (CC BY) license (<https://creativecommons.org/licenses/by/4.0/>).

Keywords: air distributor; pressure loss; resistance coefficient; flow channel structure; orthogonal test design

1. Introduction

The air conditioning system is one of the systems with high energy consumption in a ship operation, and it is also an important system for achieving people's yearning for a comfortable working and living environment. The green and energy-saving air conditioning system will make an important contribution to the energy saving and emission reduction of the shipping process and the comfort of the working and living environment [1]. Ship energy saving has become an important research topic of the shipping industry around the world. This is because ship energy saving is related to fuel saving resource and cost, environment protection, and economic benefit, etc. [2,3]. It is imperative to improve ship energy efficiency and reduce energy consumption. Scholars optimize all aspects of the ship from different angles to achieve energy-saving effects [4,5]. The air distributor is the end device of the air conditioning system [6]. It is an important part of the air conditioning system. Its function is to adjust the air supply volume and air supply temperature for the cabin and weaken the influence of the noise of the ship air conditioning system on the cabin environment. However, the high flow resistance of traditional air distributors leads to huge energy losses and poor indoor thermal comfort [7]. Because the air distributor needs to overcome factors such as pipeline resistance, air duct resistance, and protective network resistance, a certain static pressure needs to be generated during operation. Generally

speaking, the static pressure range of the air distributor is between 50 and 800 Pa, and there are different models and uses. When the air distributor is supplying air, there are many pressure factors that cause the pressure loss of the air distributor. Napreenko K S. and other scholars designed valve openings at different angles in the pipeline to study the pressure loss of the fluid after passing through the pipeline valve [8]. Through numerical simulation and a full-scale test, Gao et al. obtained a new type of low-resistance deflector, which reduces the strength of the generated vortex and the conversion efficiency of mechanical energy to internal energy by reducing the deformation of the airflow, thus reducing the local resistance by 81.4–87.16% [9–11]. Guo Y et al. experimentally explored the strategy of reshaping the traditional C-shaped channel structure to an L-shape, to reduce noise. The noise level and resistance coefficient of the improved air distributor were analyzed [12]. Ran et al. studied the resistance coefficient of the air conditioning pipeline at the elbow joint. Inspired by the structural characteristics of bat wings and humpback whale pectoral fins, bionic guide vanes were designed at the elbow joint. By setting the number of serrated teeth, the height of serrated teeth, and the width of serrated teeth, CFD prediction was used to build a test bench to verify the method. It was found that the height of serrated teeth was beneficial for reducing the local resistance coefficient. When the dimensionless height of serrated teeth was greater than 0.0625, the resistance was reduced by 9.1%, compared with that without serrated teeth [13,14]. Liang et al. of Tsinghua University designed an air conditioning system that can simultaneously adjust the ambient temperature and humidity of the room by using a three-fluid heat exchanger, and improved the situation of high energy consumption under low load conditions. Through experiments in a conference room, it was found that the energy consumption was reduced by 15.5% compared with the traditional heating and dehumidification device, and the energy consumption was reduced by 6.3% compared with the room's indoor air conditioning system [15]. Guozeng Feng of Jiangsu University of Science and Technology optimized the size and structure of the air distributor flow channel by using the method of orthogonal experimental design, screened out the effective design scheme and reduced the resistance coefficient, but did not use the comprehensive analysis method to optimize the results of the design scheme [16]. Ma et al. of Tsinghua University studied the actual performance of the clean room air conditioning system in the ventilation process and its potential improvement. The filtration method of filtering outdoor air and backflow air, respectively, reduces the airflow resistance and reduces the energy consumption of the air supply process [17]. With the increasing operating costs of the shipbuilding industry, major shipbuilding companies and ocean companies are paying more and more attention to how to achieve energy conservation and efficiency in ship operations, and regard it as the primary goal [18]. The air conditioning system in the ship is one of the largest energy consumers, consuming about 30% of the ship's energy. Therefore, the development of a low-resistance air conditioning system is a great contribution to achieving energy saving and emission reduction in ships [19].

Domestic and foreign scholars have reduced the resistance inside air conditioning ducts by studying air conditioning valves, internal duct deflectors, ventilation processes, and heat transfer methods [20–22]. However, most of the domestic and foreign scholars' research objects are for the land-based environment, and few research designs are conducted for the marine environment. Due to the harsher and more complex marine environment, the vibration frequency and amplitude of ship cabins are large. For traditional land-based research, more stable and reliable energy-saving methods are needed. In the previous air distributor structure, due to the irrationality of the flow channel the resistance coefficient of the flow channel is too high, resulting in the waste of energy, so it is necessary to design a new flow channel structure and optimize its size, to reduce the resistance during flow and ensure low energy consumption. In this paper, a new type of marine air distributor is studied, which reduces the resistance performance of the original air distributor by designing a new flow channel. In the experimental process, the number of ineffective similar schemes is greatly reduced, and the optimization scheme is obtained more quickly and effectively. In terms of structure, through orthogonal experimental design and a

comprehensive analysis method, the original dimensional structure is optimized and analyzed, and the dimensional structure with the best resistance performance is obtained, which reduces the energy loss caused by resistance.

2. Establishment of Air Distributor Model

To address the interaction between fluids and their contacts in practical engineering, it is necessary to establish the basic equation of fluid motion to determine the distribution of velocity and pressure as the fluid passes through each channel. These equations of fluid motion are derived from the three principles of mass conservation, momentum conservation, and energy conservation, and are formulated based on the specific characteristics of the fluid. Typically, these equations take the form of partial differential equations, which need to be discretized using algebraic equation-solving methods to obtain numerical solutions.

The Fluent calculation of the internal flow channel structure of the air distributor is assumed to be an incompressible viscous fluid, and conforms to the Boussinesq hypothesis. Fluid flow follows the laws of conservation of mass, momentum, energy, and turbulent transport, and the equation describing fluid flow control can be written as follows:

For the three-digit steady-state flow in this experiment, the equation can be simplified to:

$$\frac{\partial u}{\partial x} + \frac{\partial v}{\partial y} + \frac{\partial w}{\partial z} = 0 \quad (1)$$

Law of conservation of momentum:

$$\rho \frac{\partial \vec{u}}{\partial t} + \rho \vec{u} \cdot \nabla \vec{u} = -\nabla P + \nabla \tau + (\rho - \rho_\infty)g \quad (2)$$

Similarly, the equation can be simplified to:

$$\rho \left(\frac{\partial u}{\partial x} u + \frac{\partial u}{\partial y} v + \frac{\partial u}{\partial z} w \right) = \left(\frac{\partial \sigma_x}{\partial x} + \frac{\partial \tau_{xy}}{\partial y} + \frac{\partial \tau_{xz}}{\partial z} \right) + f_x \quad (3)$$

$$\rho \left(\frac{\partial v}{\partial x} u + \frac{\partial v}{\partial y} v + \frac{\partial v}{\partial z} w \right) = \left(\frac{\partial \sigma_y}{\partial x} + \frac{\partial \tau_{yx}}{\partial y} + \frac{\partial \tau_{yz}}{\partial z} \right) + f_y \quad (4)$$

$$\rho \left(\frac{\partial w}{\partial x} u + \frac{\partial w}{\partial y} v + \frac{\partial w}{\partial z} w \right) = \left(\frac{\partial \sigma_z}{\partial x} + \frac{\partial \tau_{zy}}{\partial y} + \frac{\partial \tau_{zx}}{\partial z} \right) + f_z \quad (5)$$

$$\sigma_i = -P + 2\mu \frac{\partial u_i}{\partial x_i} \quad (6)$$

$$\tau_{ij} = \mu \left(\frac{\partial u_i}{\partial x_j} + \frac{\partial u_j}{\partial x_i} \right) \quad (7)$$

Energy conservation equation:

$$\rho \frac{\partial e}{\partial t} + \rho \vec{u} \cdot \nabla e = \nabla \cdot (\lambda \nabla T) - P(\nabla \cdot \vec{u}) \quad (8)$$

$$\rho \frac{De}{DT} = -div(\rho \vec{u}) + \left[\begin{array}{l} \left(\frac{\partial(u\tau_{xx})}{\partial x} + \frac{\partial(u\tau_{xy})}{\partial y} + \frac{\partial(u\tau_{xz})}{\partial z} \right) \\ \left(\frac{\partial(v\tau_{xx})}{\partial x} + \frac{\partial(v\tau_{xy})}{\partial y} + \frac{\partial(v\tau_{xz})}{\partial z} \right) \\ \left(\frac{\partial(w\tau_{xx})}{\partial x} + \frac{\partial(w\tau_{xy})}{\partial y} + \frac{\partial(w\tau_{xz})}{\partial z} \right) \end{array} \right] + div(kgradT) + S_E \quad (9)$$

The reliability and accuracy of internal channel flow characteristic prediction depends on the correct turbulence model in the physical domain. This is because the air distributor needs to be calculated on a large scale, the flow characteristics inside the flow channel belong to the application conditions of the $k-\varepsilon$ model, and the $k-\varepsilon$ model is consistent with

the experimental values. In the best case, the error is less than 5.5%. Therefore, the k - ε model is selected to predict the drag performance and aerodynamic noise of the air distributor. The Reliable k - ε model in Fluent is an improvement of the standard k - ε model. It is based on the theory of the multi-scale turbulence model. By adding new equations to describe turbulent motion, the prediction accuracy of the model is improved. The Reliable K model is more suitable for a high Reynolds number flow and more complex flow fields, such as the turbulent flow and non-equilibrium boundary layer.

Using the k - ε model, the rated working condition of the air distributor is 600 Pa, 250 m³/h, and the resistance performance and noise performance of the air distributor under different working conditions are positively correlated with static pressure, so this optimization only needs to calculate the resistance performance and noise performance of the air distributor under the rated working conditions. Since the outlet of the air distributor is located in the cabin or building, the pressure of these working conditions is generally atmospheric pressure, and the pressure of the outlet of the air distributor in the Fluent is relative pressure, so the outlet boundary condition is set to 0 Pa.

The Reliable k - ε model:

$$\frac{\partial}{\partial t}(pk) + \frac{\partial}{\partial x_i}(\rho k u_i) = \frac{\partial}{\partial x_i} \left[\left(\mu + \frac{\mu_t}{\sigma_k} \right) \frac{\partial k}{\partial x_j} \right] + G_k + G_b - \rho \varepsilon - Y_m + S_k \quad (10)$$

$$\frac{\partial}{\partial t}(p\varepsilon) + \frac{\partial}{\partial x_i}(\rho \varepsilon u_i) = \frac{\partial}{\partial x_i} \left[\left(\mu + \frac{\mu_t}{\sigma_\varepsilon} \right) \frac{\partial \varepsilon}{\partial x_j} \right] + C_{1\varepsilon} \frac{\varepsilon}{k} (G_k) + C_{3\varepsilon} G_b - C_{2\varepsilon} \rho \frac{\varepsilon^2}{k} - S_\varepsilon \quad (11)$$

2.1. Grid Independence Verification

Grid independence verification is typically a balance between simulation accuracy and computational efficiency. A mesh that is too fine will increase computational costs, while a mesh that is too coarse will result in inaccurate simulation results. Fluent meshing is utilized to partition the polyhedral mesh of the original air distributor model, followed by conducting CFD numerical simulations using Fluent 2022R1 software to analyze the airflow within the air distributor flow channels. In this study, eight different grid configurations are employed, with the resistance coefficient serving as the monitored value. See Figure 1 below. The results indicate that, as the number of grids increases, the calculated resistance coefficient gradually stabilizes and becomes unaffected by the grid density. Hence, it can be concluded that the calculation results are reliable. Based on these findings, a grid configuration of 400,000 is chosen for the simulation calculation.

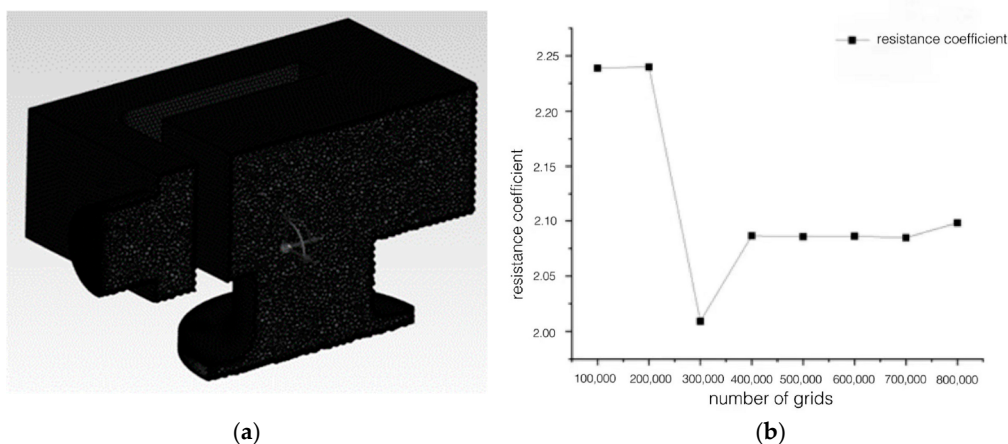


Figure 1. Computational domain and results for the inner runner of the air distributor. (a) Inner flow channel computational grid. (b) Different grid calculation results.

2.2. Optimization Scheme of Internal Flow Channel of U-Type Air Distributor

The internal flow channel structure of the U-shaped air distributor is shown in Figure 2. When studying the influence of the new U-shaped flow channel on the resistance coefficient of the air distributor, there are four different size structures in the U-shaped flow channel, and the size of these structures directly affects the resistance coefficient of the air distributor. However, in order to further reduce the resistance coefficient of the air distributor, it is necessary to optimize the structure size of the U-shaped flow channel.

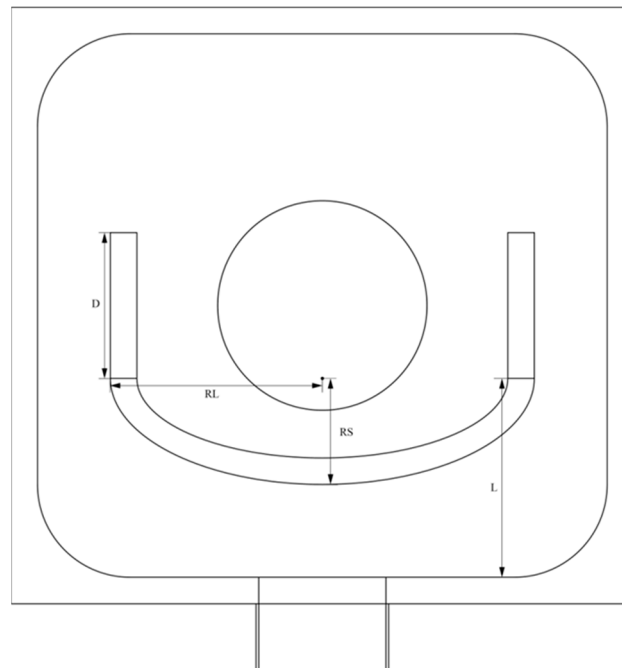


Figure 2. Model diagram of the flow computational domain inside a U-shaped air distributor.

Under the rated condition (600 Pa static pressure, 250 m³/h), one flow channel parameter is changed respectively, and the other three parameters are kept as the initial values. The simulation analysis results for the resistance coefficient are shown in Figure 3. The results show that the RL value has the greatest influence on the resistance coefficient. To reduce the resistance coefficient, RL, RS, and D must be properly reduced, and L must be increased.

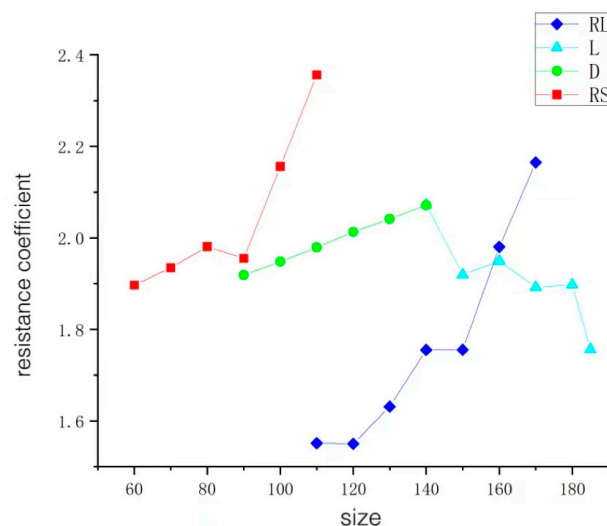


Figure 3. Influence of four structural parameters on resistance coefficient.

The U-shaped flow channel still uses the orthogonal experimental design method mentioned above to optimize the structural parameters of the new U-shaped flow channel in order to further reduce the resistance coefficient of the air distributor. According to the steps of orthogonal test design in the previous article, L16(4⁴), factor level table and table head design table were finally selected. The design schemes are shown in Tables 1–3.

Table 1. U-shape air distributor factor level table.

Level	Factor			
	RS	RL	L	D
1	60	110	160	90
2	65	115	155	95
3	70	120	150	100
4	75	125	145	105

Table 2. Design of header for orthogonal test of flow structure parameters of U-shaped air distributor.

Factor	RS	RL	L	D
L ₁₆ (4 ⁴)	1	2	3	4

Table 3. Test design table of structural parameters of U-shaped air distributor.

Column Number	1	2	3	4
Experimental Serial Number	RS	RL	L	D
scheme 1	(1) 60	(1) 110	(1) 160	(1) 90
scheme 2	(1) 60	(2) 115	(2) 155	(2) 95
scheme 3	(1) 60	(3) 120	(3) 150	(3) 100
scheme 4	(1) 60	(4) 125	(4) 145	(4) 105
scheme 5	(2) 65	(1) 110	(2) 155	(3) 100
scheme 6	(2) 65	(2) 115	(1) 160	(4) 105
scheme 7	(2) 65	(3) 120	(4) 145	(1) 90
scheme 8	(2) 65	(4) 125	(3) 150	(2) 95
scheme 9	(3) 70	(1) 110	(3) 150	(4) 105
scheme 10	(3) 70	(2) 115	(4) 145	(3) 100
scheme 11	(3) 70	(3) 120	(1) 160	(2) 95
scheme 12	(3) 70	(4) 125	(2) 155	(1) 90
scheme 13	(4) 75	(1) 110	(4) 145	(2) 95
scheme 14	(4) 75	(2) 115	(3) 150	(1) 90
scheme 15	(4) 75	(3) 120	(2) 155	(4) 105
scheme 16	(4) 75	(4) 125	(1) 160	(3) 100

In order to optimize the flow channel parameters of the air distributor, multiple variables need to be considered, including RS, RL, L, and D. If a comprehensive test is carried out for each parameter, 256 schemes need to be tested, so the amount of calculation and the workload are very large. However, by using the orthogonal table, the test scheme can be designed more efficiently, and only 16 tests are needed. However, these tests can clearly analyze the design scheme that has the greatest influence on the resistance coefficient and other indicators, and then use the comprehensive analysis method to obtain the internal flow channel design scheme with the best optimization effect. Using this design method and a comprehensive data analysis method can help find the optimal parameter combination more quickly, thus reducing the calculation and workload.

3. Optimization Results of Internal Flow Channel Resistance of U-Shaped Air Distributor

According to Table 4, the three-dimensional modeling software is used to model the sixteen schemes, and the pre-processing software is used to extract the fluid domain to

obtain the internal flow channel structure of the air distributor that needs to be calculated by CFD. The Fluent meshing is used to mesh the internal flow channel structure of the air distributor. After the above mesh independence verification, the optimization process will mesh the optimized air distributor structure, according to the above mesh setting method.

Table 4. Resistance coefficient and differential pressure of each structure of the air distributor.

Experimental Serial Number	RS	RL	L	D	Drag Coefficient	Pressure Difference
scheme 1	60	110	160	90	1.418	60.7
scheme 2	60	115	155	95	1.449	61.99
scheme 3	60	120	150	100	1.462	62.56
scheme 4	60	125	145	105	1.436	61.44
scheme 5	65	110	155	100	1.438	61.53
scheme 6	65	115	160	105	1.446	61.86
scheme 7	65	120	145	90	1.492	63.86
scheme 8	65	125	150	95	1.422	60.85
scheme 9	70	110	150	105	1.484	63.48
scheme 10	70	115	145	100	1.505	64.41
scheme 11	70	120	160	95	1.481	63.37
scheme 12	70	125	155	90	1.445	61.81
scheme 13	75	110	145	95	1.508	64.50
scheme 14	75	115	150	90	1.502	64.25
scheme 15	75	120	155	105	1.485	63.52
scheme 16	75	125	160	100	1.422	60.80

The model after meshing is numerically calculated using Fluent, and is set according to the model verified above, to ensure the accuracy and credibility of the optimized prediction results. Because the rated working condition of the air distributor is 600 Pa, 250 m³/h, and the resistance performance and noise performance of the air distributor under different working conditions are positively correlated with the static pressure, this optimization only needs to calculate the resistance performance and noise performance of the air distributor under the rated working condition.

Figure 4, drawn from the calculated data, shows intuitively that the resistance coefficient and pressure loss of scheme 8 are the lowest. As shown in Figure 4a, compared with the original scheme, the resistance coefficient of the new U-shaped channel design is significantly reduced, to below 1.6. As shown in Figure 4b, the pressure loss of the new flow channel design scheme is reduced from the original 106.84 Pa to below 65 Pa; the resistance coefficient of scheme 1 is reduced to 1.418, and the pressure difference is reduced to 60.7 Pa.

In order to verify the results of the optimal scheme in the original 256 schemes, the results of the scheme are analyzed by means of visual analysis. The conclusions of the analysis are shown in Table 4 and Figure 4.

In Table 5 and Figure 5, it can be concluded that RL has the greatest influence on the resistance coefficient, and is the main influencing factor, followed by L, RS, and D, which has the least influence on the resistance coefficient. In Figure 5a, it can be seen that the resistance coefficient is the lowest when RS = 60 mm. In Figure 5b, it can be seen that the resistance coefficient is the lowest when RL = 125 mm. In Figure 5c, it can be seen that L is negatively correlated with the resistance coefficient, and the resistance coefficient is the smallest when L = 160 mm. From Figure 5d, it can be seen that when D is 100 mm, the structure size with the lowest resistance coefficient can be obtained. Finally, the scheme with the lowest resistance coefficient can be obtained when S = 60 mm, RL = 125 mm, L = 160 mm, and D = 100 mm.

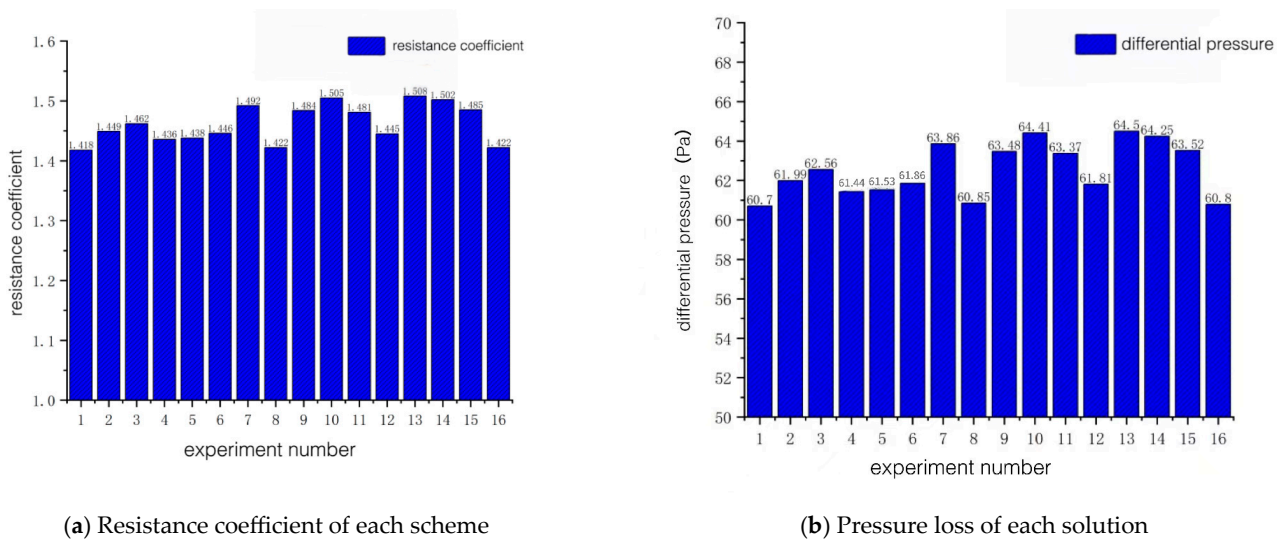


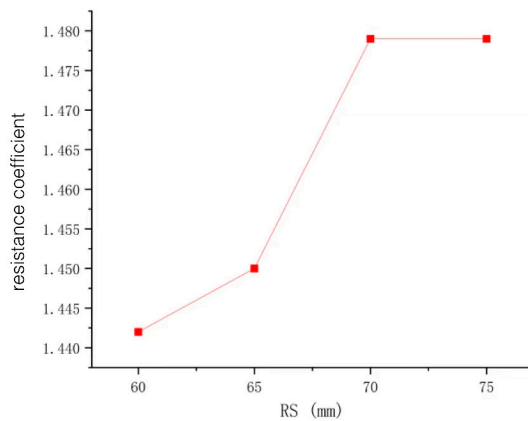
Figure 4. Resistance coefficient and pressure loss for each scheme.

Table 5. Combined comparison of resistance coefficient results.

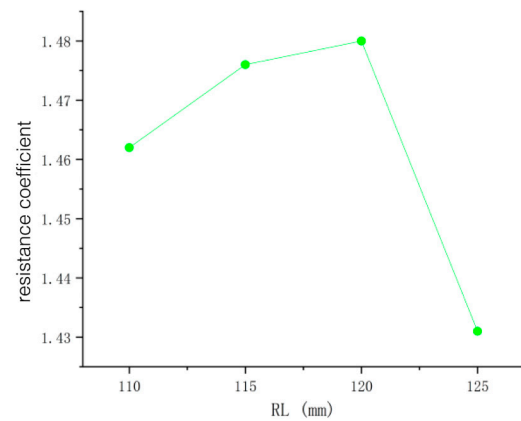
Level	RS Average Resistance Coefficient	RL Average Resistance Coefficient	L Average Resistance Coefficient	D Average Resistance Coefficient
1	1.442	1.462	1.486	1.464
2	1.450	1.476	1.468	1.465
3	1.479	1.480	1.454	1.457
4	1.479	1.431	1.442	1.463
Influence	0.037	0.049	0.044	0.008
Influence ranking	3	1	2	4

Through orthogonal experimental design and a comprehensive analysis method, the optimal size structure of resistance performance is obtained. By using three-dimensional modeling software and Fluent solution, the resistance coefficient of the new structure is 1.375 and the pressure loss is 56.87 Pa. Compared with scheme 1, the resistance coefficient and pressure loss are reduced by 3.03% and 6.29%, respectively. It can be seen in Figure 6a that, due to the change in the structure of the internal deflector, the air flow obtained by the original direct impact on the deflector plane flows out more evenly from both sides of the deflector under the action of the new deflector, thus reducing the pressure difference between the inlet and outlet.

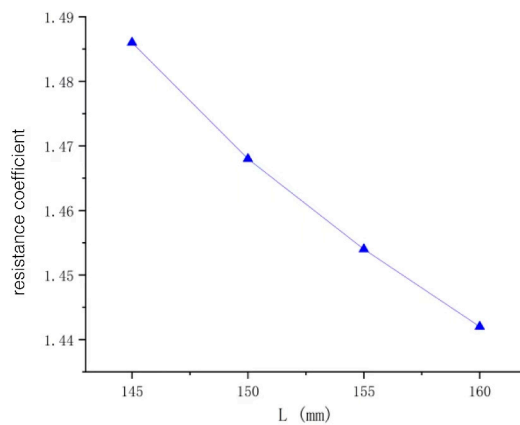
It can be seen from Figure 6b that the velocity mutation area of the new structure is reduced, the flow dead zone at the front end is significantly reduced, compared with the original structure, and the eddy current zone is reduced, compared with the original structure. From Figure 6c,d, it can be seen that the internal streamline at the inlet is not entangled too much in the front area, and can pass through the inlet area smoothly. After changing the direction of fluid flow through the deflector and the rear wall, the flow of the air on the upper side of the outlet is more uniform. Because the new structure is rounded to the original angular area, the air flow is smoother when it flows inside, so there is no vortex, thus reducing the drag coefficient and aerodynamic noise. It can evenly send the air out of the air outlet to achieve the purpose of energy saving and emission reduction, so that the staff in the room can work in a comfortable environment.



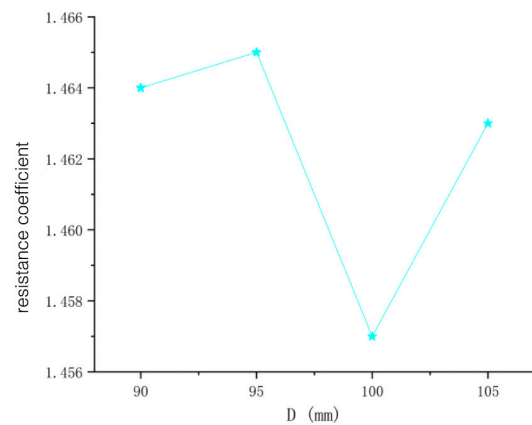
(a) RS level mean value



(b) RL level mean value



(c) L level mean value



(d) D level mean value

Figure 5. The mean value diagram of each factor of resistance coefficient.

Based on the above experiments and analysis, it can be seen that, compared with the original scheme [16], the resistance coefficient of the runner design is significantly reduced, to less than 1.6. At the same time, the pressure loss of the new flow channel design scheme was reduced from 106.84 Pa to less than 65 Pa, and the lowest result was that the drag coefficient was reduced to 1.418 and the pressure difference was reduced to 60.7 Pa. On this basis, the influence of each influencing factor on the drag coefficient is analyzed again, and finally the analysis shows that the scheme with the lowest resistance coefficient can be obtained when $S = 60$ mm, $RL = 125$ mm, $L = 160$ mm, and $D = 100$ mm. By using 3D modeling software and Fluent, the new structure can be obtained with a drag coefficient of 1.375 and a pressure loss of 56.87 Pa. Compared with the drag coefficient of 1.414 and the pressure difference of 60.7 Pa obtained in the first optimization, the drag coefficient and pressure loss were reduced by 3.03% and 6.29%, respectively. And from the pressure cloud diagram, it can be clearly seen that the pressure difference between the inlet and outlet of the air distributor is reduced, and the internal airflow is more uniform. The corners of the original structure are more rounded, which reduces the drag coefficient and reduces aerodynamic noise. In this way, it can reduce the loss of air volume and the energy consumption of ship air conditioning, and it also reduces indoor energy waste.

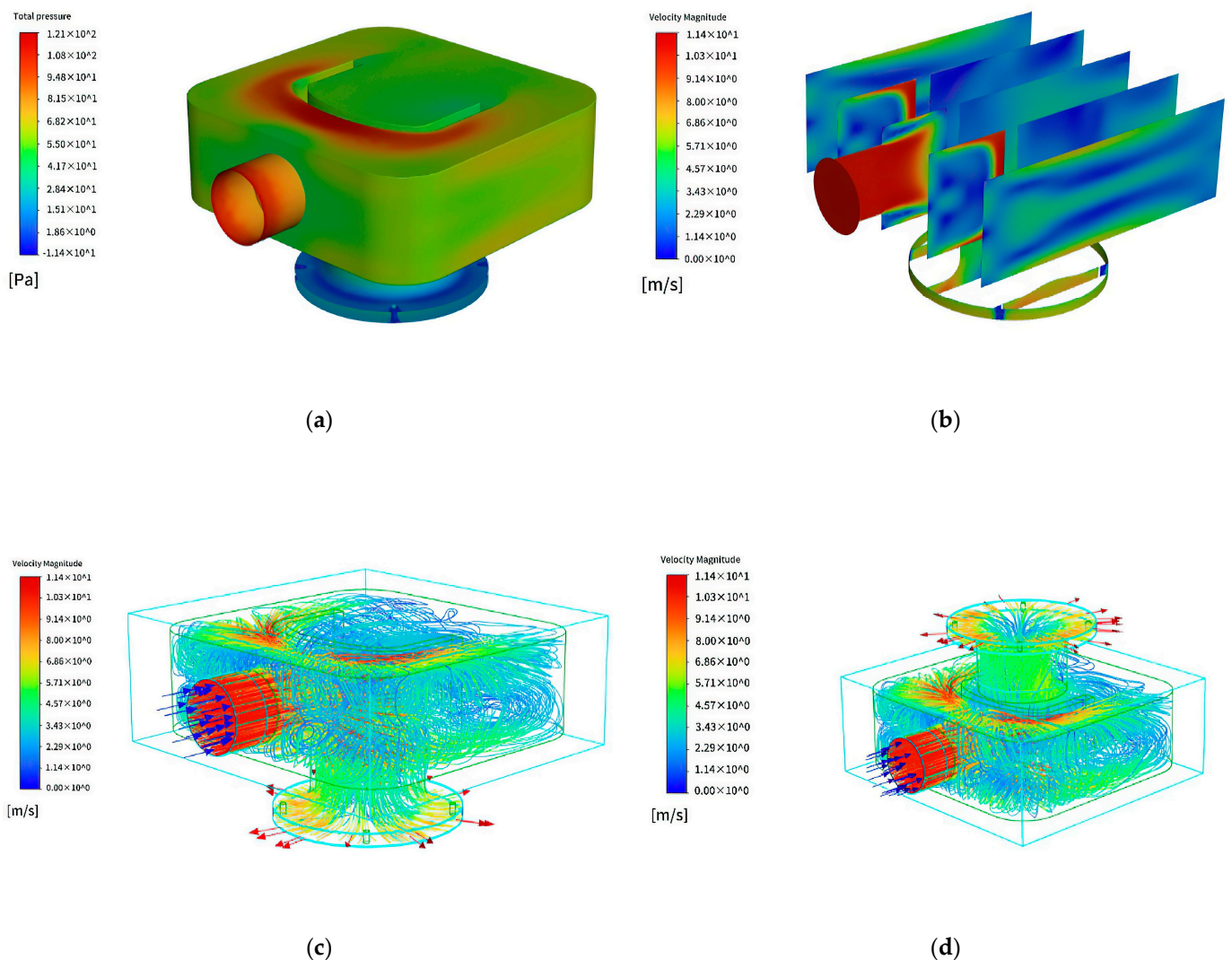


Figure 6. Numerical simulation results of U-shaped air distributor. (a) Air distributor pressure cloud diagram. (b) Wind speed cloud diagram. (c) The internal streamline diagram of the air distributor (positive axis mapping). (d) Internal streamline diagram of air distributor (reverse axis mapping).

4. Conclusions

It can be seen from the above experiments and analysis that the air distributor utilizes a U-shaped structure, which effectively reduces flow dead zones and promotes a more moderate and smooth flow pattern. Through orthogonal test design and comprehensive analysis, the resistance coefficient of the new structure is determined to be 1.375, with a pressure loss of 56.87 Pa. When compared to the initial scheme, whose resistance coefficient is 1.418 and pressure loss is 60.7 Pa, the resistance coefficient and pressure loss are reduced by 3.03% and 6.29%, respectively. The application of orthogonal experimental design analysis provides theoretical guidance for the design and manufacturing of air distributors, thereby optimizing their structural design. This method saves a significant amount of computing power and design time for engineers and technicians. The number of ineffective and similar protocols is greatly reduced during the experiment, and it also saves time and reduces experimental consumables. What is more, it saves energy. In terms of structure, through orthogonal experimental design and the comprehensive analysis method, the original dimensional structure is optimized and analyzed, and the dimensional structure with the best resistance performance is obtained, which reduces the energy loss caused by resistance. Due to the widespread use of independent power grids in the marine industry during operation, and because of the complexity of its environment, the energy

consumption of ship electrical systems is relatively high for a ship operation. As a high-energy-consuming piece of equipment on a ship, the air conditioning system is very important in the application of ship electrical equipment technology, for reducing its energy consumption without affecting its normal work. Through the experiment and analysis of this paper, theoretical guidance can be put forward for the manufacture of air distributors, reducing the resistance loss and wind energy waste during the operation of ship air conditioners, and reducing the energy consumption of ship air conditioners.

Author Contributions: Conceptualization, Z.W. and J.W.; methodology, J.X. and J.W.; software, Z.W.; validation, J.X., J.W. and Z.W.; formal analysis, Z.W.; investigation, Z.W.; resources, J.X. and J.W.; data curation, Z.W.; writing—original draft preparation, Z.W.; writing—review and editing, Z.W. and J.W. All authors have read and agreed to the published version of the manuscript.

Funding: This research was supported by the Public Service Platform Project of Shanghai Science and Technology Commission (20DZ2292200).

Data Availability Statement: No new data were created.

Conflicts of Interest: The authors declare no conflict of interest.

Abbreviations

Nomenclature

ρ	Density (kg/m ³)
t	Time (s)
σ	Normal stress (N/m)
τ	Tangential stress (N/m)
div	Mathematical operator
$grad$	Mathematical operator
e	Special internal energy (J/kg)
g	Gravity (m/s ²)
i, j	Symbol representing any spatial coordinate subscript
k	Thermal conductivity (W/(m·k))
p	System pressure (Pa)
S_E	Source item (N/m ³)
u	Velocity in the x-direction (m/s)
v	Velocity in the y-direction (m/s)
w	Velocity in the z-direction (m/s)
G_K	Turbulent kinetic energy generated by average velocity gradient (J)
G_b	Turbulent kinetic energy generated by buoyancy (J)
Y_m	Contribution rate of pulsation expansion in turbulence to total dissipated power
$C_{1\varepsilon}$	Constant
$C_{2\varepsilon}$	Constant
$C_{3\varepsilon}$	Constant
a_k	Turbulent Prandtl number of k
a_ε	Turbulent Prandtl of ε

References

1. Wu, S.; Cheng, Y.T.; Ma, Q. Discussion on ship energy-saving in low carbon economy. *Procedia Eng.* **2011**, *15*, 5259–5262. [[CrossRef](#)]
2. Korkut, E. A case study for the effect of a flow improvement device (a partial wake equalizing duct) on ship powering characteristics. *Ocean Eng.* **2006**, *33*, 205–218. [[CrossRef](#)]
3. Wang, Y.F.; Li, K.P.; Xu, X.M.; Zhang, Y.R. Transport energy consumption and saving in China. *Renew. Sust. Energy. Rev.* **2014**, *29*, 641–655. [[CrossRef](#)]
4. Yu, J.W.; Lee, M.K.; Kim, Y.I.; Suh, S.B.; Lee, I.W. An optimization study on the hull form and stern appendage for improving resistance performance of a coastal fishing vessel. *Appl. Sci.* **2021**, *11*, 6124. [[CrossRef](#)]
5. Rezaei, S.; Bamdadinejad, M.; Ghassemi, H. Numerical simulations of the hydrodynamic performance of the propeller with wake equalizing duct behind the ship. *Sci. Iran.* **2022**, *29*, 2332–2348. [[CrossRef](#)]
6. Huang, W.; Zhu, L.; Liang, Y.; Wang, Q.; Chen, W. Design and Simulation Analysis of Acoustic Performance of Marine Low Noise Air Distributors. *Noise Vib. Control.* **2021**, *41*, 127–132.

7. Feng, G.; Lei, S.; Guo, Y.; Shi, D.; Shen, J.B. Optimisation of air-distributor channel structural parameters based on Taguchi orthogonal design. *Case Stud. Therm. Eng.* **2020**, *21*, 100685. [[CrossRef](#)]
8. Napreenko, K.S.; Lamtyugina, A.V. Hydraulic losses optimization methods used in air conditioning system valve design for different closure angles. *IOP Conf. Ser. Mater. Sci. Eng.* **2021**, *1027*, 012022. [[CrossRef](#)]
9. Gao, R.; Fang, Z.; Li, A.; Liu, K.; Yang, Z.; Cong, B. A novel low-resistance tee of ventilation and air conditioning duct based on energy dissipation control. *Appl. Therm. Eng.* **2018**, *132*, 790. [[CrossRef](#)]
10. Zhang, S.C.; Zhang, Y.L.; Fang, Z.M. Numerical simulation and analysis of ball valve three-dimensional flow based on CFD. *IOP Conf. Ser. Earth Environ. Sci.* **2012**, *15*, 052024. [[CrossRef](#)]
11. Cui, B.L.; Ma, G.W.; Wang, H.J.; Lin, Z.; Sang, Z.H. Influence of valve core structure on flow resistance characteristics and internal flow field of throttling stop valve. *J. Mech. Eng.* **2015**, *51*, 178–184. [[CrossRef](#)]
12. Guo, Y.; Feng, G.; Lei, S.; Meng, B.; Xu, Y. Experimental study of aerodynamic noise performance of improved air distributor for ships. *Adv. Mech. Eng.* **2021**, *13*, 16878140211001239. [[CrossRef](#)]
13. Gao, R.; Guo, W.; Yang, C.; Wang, M.; Zhang, S.; Zhou, H.; Li, A. Truncation method for calculating the resistance of ventilation air-conditioning duct systems under nonfully developed flow boundary conditions. *Build. Simul.* **2021**, *14*, 1237–1249. [[CrossRef](#)]
14. Ai, Z.T.; Mak, C.M. Pressure losses across multiple fittings in ventilation ducts. *Sci. World J.* **2013**, *2013*, 195763. [[CrossRef](#)] [[PubMed](#)]
15. Liang, C.; Wang, Y.; Li, X. Energy-efficient air conditioning system using a three-fluid heat exchanger for simultaneous temperature and humidity control. *Energy. Convers. Manag.* **2022**, *270*, 116236. [[CrossRef](#)]
16. Feng, G.; Wang, Y.; Gu, X.; Xu, T.; Gu, C.; Xia, Y.; Han, G.; Luan, F. An Optimization Design Method of Internal Flow Channel Structure of Air Distributor Based on Orthogonal Test. Patent CN113536640A, 22 October 2021.
17. Ma, Z.; Guan, B.; Liu, X.; Zhang, T. Performance analysis and improvement of air filtration and ventilation process in semiconductor clean air-conditioning system. *Energy Build.* **2020**, *228*, 110489. [[CrossRef](#)]
18. Li, C.; Li, Y. Energy Saving Design of Ship Air Conditioning System. *Public Util. Des.* **2016**, *77*. [[CrossRef](#)]
19. Lei, S. *Study on Resistance and Aerodynamic Noise Performance of Low Noise VAV Marine Air Distributor*; Jiangsu University of Science and Technology: Zhenjiang, China, 2020; pp. 1–2.
20. Zhang, K.; Wu, D.; Wang, H.; Li, J.; Feng, Z.; Zhu, J.; Lai, Z. Investigation of Effects of Slider Structure on the Reversing Performance of Four-Way Reversing Valve. *Processes* **2023**, *11*, 1538. [[CrossRef](#)]
21. Li, B.; Lu, Q.; Jiang, B.; Yang, J.; Wang, J.; Xie, J. Effects of Outer Edge Bending on the Aerodynamic and Noise Characters of Axial Fan for Air Conditioners. *Processes* **2022**, *10*, 686. [[CrossRef](#)]
22. Yang, S.; Zhao, Z.; Zhang, Y.; Chen, Z.; Yang, M. Effects of Fin Arrangements on Thermal Hydraulic Performance of Supercritical Nitrogen in Printed Circuit Heat Exchanger. *Processes* **2021**, *9*, 861. [[CrossRef](#)]

Disclaimer/Publisher’s Note: The statements, opinions and data contained in all publications are solely those of the individual author(s) and contributor(s) and not of MDPI and/or the editor(s). MDPI and/or the editor(s) disclaim responsibility for any injury to people or property resulting from any ideas, methods, instructions or products referred to in the content.